STATISTICAL COMBINATION OF UNCERTAINTIES

PART 1

DECEMBER, 1979

POWER SYSTEMS
COMBUSTION ENGINEERING, INC.

LEGAL NOTICE

THIS REPORT WAS PREPARED AS AN ACCOUNT OF WORK SPONSORED BY COMBUSTION ENGINEERING, INC. NEITHER COMBUSTION ENGINEERING NOR ANY PERSON ACTING ON ITS BEHALF:

A. MAKES ANY WARRANTY OR REPRESENTATION, EXPRESS OR IMPLIED INCLUDING THE WARRANTIES OF FITNESS FOR A PARTICULAR PURPOSE OR MERCHANTABILITY, WITH RESPECT TO THE ACCURACY, COMPLETENESS, OR USEFULNESS OF THE INFORMATION CONTAINED IN THIS REPORT, OR THAT THE USE OF ANY INFORMATION, APPARATUS, METHOD, OR PROCESS DISCLOSED IN THIS REPORT MAY NOT INFRINGE PRIVATELY OWNED RIGHTS; OR

B. ASSUMES ANY LIABILITIES WITH RESPECT TO THE USE OF, OR FOR DAMAGES RESULTING FROM THE USE OF, ANY INFORMATION, APPARATUS, METHOD OR PROCESS DISCLOSED IN THIS REPORT.

CEN-124(B)-NP

STATISTICAL COMBINATION OF UNCERTAINTIES METHODOLOGY

PART 1: C-E CALCULATED LOCAL POWER DENSITY AND THERMAL MARGIN/LOW PRESSURE LSSS FOR CALVERT CLIFFS UNITS I AND II

ABSTRACT

This report describes the methods used to statistically combine uncertainties for the C-E calculated Local Power Density (LPD) LSSS and Thermal Margin/Low Pressure (TM/LP) LSSS for Calvert Cliffs Units I and II.

A detailed description of the uncertainty probability distributions and the stochastic simulation techniques used is presented. The total uncertainties presented in this report are expressed in percent overpower (P_{fdn}, P_{fdl}) units, assigned to the LPD LSSS and the TM/LP LSSS at the 95/95 probability/confidence limit.

TABLE OF CONTENTS

TABLE OF CONTENTS (Continued)

LIST OF TABLES

LIST OF FIGURES

DEFINITION OF ACRONYMS AND ABBREVIATIONS

ACU	Axial shape index calibration uncertainty
AOO	Anticipated Operational Occurrence(s)
APU,TPU	Processing uncertainty
ARO	All rods out
ASI	Axial shape index after application of uncertainties
ASI_{DNB}^{LSSS}	Axial shape index after inclusion of the DNB LSSS uncertainties
ASI_{LHR}^{LSSS}	Axial shape index after inclusion of LHR LSSS Uncertainties
B	Unless specifically defined in context as representing ΔT Power, B is used interchangeably with Q, core power.
B_{DNB}	P_{fdn} after application of uncertainties
B_{LHR}	P_{fdl} after application of uncertainties
B_{LHR_h}	LHR overpower including uncertainties
B^{LSSS}	Power limit for LHR LSSS
B_{opm}	Available overpower margin
B_{opmo}	Reference B_{opm} for calculating the constants in the TM/LP trip equation
B_{DNB}^{LSSS}	Power level after inclusion of DNB LSSS uncertainties and allowances.
B_{LHR}^{LSSS}	Power level after inclusion of linear heat rate LSSS uncertainties and allowances.
$B_{opm_{k(h)}}$	k^{th} (h^{th}) simulated value of overpower margin.
$\Delta B_{opm_{k(h)}}$	k^{th} (h^{th}) value of sampled overpower uncertainty due to axial shape index uncertainties
BMU	Power measurement uncertainty
$BMU_{k(h)}$	Value of the power measurement uncertainty sampled by SIGMA in trial k(h).
BOC	Beginning of Cycle
CEA	Control Element Assembly
CECOR	Computer code used to monitor core power distributions
CETOP	Computer code used to determine the overpower limits due to thermal-hydraulic conditions
CE-1 DNBR	DNB Ratio calculated by the TORC/CE-1 correlation

DBE	Design Basis Event(s)
Di	Value of simulation point i
DNB	Departure from Nucleate Boiling
DNBR	Departure from Nucleate Boiling Ratio
EOC	End of Cycle
F	Primary coolant flow rate
f	Number of degrees of freedom
F^{DNB}	Coolant flow used in the generation of (P_{fdn}, I_p) ordered pairs of data
F_e	Engineering factor on local heat flux
F_q, F_q^n	Synthesized three-dimensional core power peak
F^P	Planar radial peaking factor
F_R	Integrated radial peaking factor
H	Height of core
$\bar{I}$	Core average axial shape index
I_e	External shape index
I_i	Axial shape index for the i^{th} assembly
I_p	Peripheral axial shape index
$\bar{I}^Q$	QUIX-calculated core average axial shape index
I_p^Q	QUIX-calculated I_p
$I_p^Q(RSF)$	QUIX calculated value of I_p using the rod shadowing factor method
$\bar{I}^R$	ROCS-calculated core average axial shape index
I_p^R	ROCS-calculated I_p
$I_p^R(AWF)$	ROCS power distribution based values of I_p using the assembly weighting factor method
$I_p^R(RSF)$	ROCS power distribution based values of I_p using the rod shadowing factor method
I_p^C	I_p calculated by CECOR
$\bar{I}^C$	$\bar{I}$ calculated by CECOR
L	Power in lower half of core
LCO	Limiting Condition(s) for Operation
LHS	Latin Hypercube Sampling
LHR	Linear Heat Rate
LPD	Local Power Density
LPD LSSS	Local power density LSSS also called axial flux offset LSSS

LSSS	Limiting Safety System Setting(s)
MDNBR	Minimum DNBR
MOC	Middle of Cycle
Mwt	Megawatt(s) thermal
MTC	Moderator Temperature Coefficient
N	Sample size
NSSS	Nuclear Steam Supply System(s)
P	Reactor coolant system pressure
$\bar{P}(J)$	Average power in axial node J
P_i	Axially integrated power of assembly i
P_{fdl}	Power to the fuel design limit on fuel centerline melt
P_{fdl_h}	Value of P_{fdl} from simulation h
P^{DNB}	Pressure used in calculating the (P_{fdn}, I_p) ordered pairs of data
P_{fdn}	Power to DNBR SAFDL
P_{fdn_k}	Overpower from CETOP for the sampled input parameters in simulation k
P_{var}	Variable low pressure trip limit
P_{var}^{DNB}	Variable pressure to achieve DNB at the LSSS limit
$P_{var}^{LSSS,DNB}$	Variable pressure to achieve DNB at the LSSS limit including uncertainties
PDIL	Power Dependent CEA Group Insertion Limit
PMU	Pressure Measurement Uncertainty
PU	Uncertainty in predicting local core power at the fuel design limit
$\bar{P}(x)$	Normalized power level at core height x
Q	Core power, auctioneered higher of flux power or ΔT power
QUIX	Computer code used to solve the 1 dimensional neutron diffusion equation
RCS	Reactor Coolant System
RDT	Pressure equivalent of the total trip unit and processing delay time for the DBE exhibiting the most rapid approach to the SAFDL on DNBR
ROCS	Coarse mesh code for calculating power distributions
RPS	Reactor Protection System
RSU	Peripheral shape index uncertainty

R(x)	Rod shadowing factor at core height x
S	Sample standard deviation
SAFDL	Specified Acceptable Fuel Design Limit(s)
SAU	Shape annealing factor uncertainty
SC	Approved credit in lieu of statistical combination of uncertainties
SCU	Statistical Combination of Uncertainties
SIGMA	Stochastic Simulation Code
SMLS	Statistically combined uncertainties applicable to the Local Power density LSSS
T_{AZ}	Azimuthal tilt allowance
T_c, T_{in}	Reactor coolant cold leg, inlet temperature
T_{in}^{DNB}	Inlet coolant temperature used in the calculation of (P_{fdn}, I_p) ordered pairs of data
$T_{in}^{LSSS,DNB}$	Final inlet coolant temperature for LSSS calculation
T_h	Reactor coolant hot leg temperature
TMLL	Thermal Margin Limit Line(s)
TM/LP	Thermal Margin/Low Pressure
TMU	Temperature measurement uncertainty
TORC/CE-1	Thermal hydraulic calculational model including CE-1 critical heat flux correlation
TPD	Allowance for Transient Power Decalibration
TPU	Trip processing uncertainty
U	Power in upper half of core
VHPT	Variable High Power Trip
W_{avg}	Core average linear heat rate
W_{clm}	Peak generated linear heat rate limit corresponding to the SAFDL on fuel centerline melt
Wi	Weighting factor of assembly i
x	Axial position
$\bar{X}$	Sample mean
Z_i	i^{th} value of a normally distributed random variable with zero mean and unit standard deviation
α	Shape annealing factor

$(\alpha),(\beta),$ (γ)	Coefficients in the P_{var}^{DNB} equation
ζ	Population mean
σ	Population standard deviation
μ	Axial shape index correction term
$\mu^{Q}(r)$	[ ]
μ^{R}	[ ]
μ^{C}	[ ]
μ_{S}	[ ]
χ_{f}^{2}	Chi-squared deviate with f degrees of freedom

1.0 INTRODUCTION

1.1 PURPOSE

The purpose of this report is to describe a method for statistically combining the uncertainties involved in the analog protection and monitoring system setpoints. The following uncertainties are considered:

1. Uncertainty in predicting integrated radial pin power
2. Uncertainty in predicting local core power density
3. Power measurement uncertainty
4. Shape annealing factor uncertainty
5. Shape index separability uncertainty
6. Axial shape index calibration uncertainty
7. Processing uncertainty
8. Flow measurement uncertainty
9. Pressure measurement uncertainty
10. Temperature measurement uncertainty

1.2 BACKGROUND

1.2.1 Protection and Monitoring System

The analog protection and monitoring systems in operation on the Combustion Engineering Nuclear Steam Supply Systems have been designed to assure safe operation of the reactor in accordance with the criteria established in 10 CFR 50, Appendix A. This is demonstrated in the Final Safety Analysis Report (FSAR) and subsequent reload licensing amendments.

This is achieved by specifying:

1. Limiting Safety System Settings (LSSS) in terms of parameters directly monitored by the Reactor Protection System (RPS); and
2. Limiting Conditions for Operation (LCO) for reactor system parameters.
3. LCOs for equipment performance

The LSSS, combined with the LCO, established the thresholds for protection system action to prevent exceeding acceptable limits during Design Basis Events (DBE) where changes in DNBR and LHR are important. The limits addressed by the RPS are:

1. The reactor fuel shall not experience centerline melt; and
2. The departure from nucleate boiling ratio shall have a minimum allowable limit corresponding to a 95% probability at a 95% confidence level that DNB will not occur.

The RPS trips jointly provide protection for all AOOs. The RPS providing primary protection from centerline melt is the Local Power Density (LPD) LSSS. The RPS providing primary DNB protection is the Thermal Margin/Low Pressure (TM/LP) LSSS.

The design of the RPS requires that correlations including uncertainties be applied to express the LSSS in terms of functions of monitored parameters.

These functions are the trip limits which are then set into the RPS. A list of parameters which affect the calculation of limits for linear heat rate and DNB protection is shown in Table 1-1. A more detailed discussion of C-E setpoint methodology may be found in Reference 1-1.

1.2.2 Previous Uncertainty Evaluation Procedure

The methods previously in use for the application of uncertainties to the subject limits are presented in Reference 1-1 and summarized in Appendix B.

As noted in Reference 1-1 these methods assume that all applicable uncertainties occur simultaneously in the most adverse direction even though not all of the uncertainties are systematic; some are random and some contain both systematic and random characteristics. This assumption is extremely conservative. As described in References 1-2, partial credit has been allowed in view of the existence of this conservatism. This report documents the methodology used to statistically combine uncertainties explicitly in lieu of the credit previously used.

1.3 REPORT SCOPE

The scope of this report encompasses the following objectives:

1. To define the methods used to statistically combine uncertainties applicable to the Thermal Margin/Low Pressure (TM/LP) and Local Power Density (LPD) LSSS;

2. To evaluate the aggregate uncertainties as they are applied in the determination of the TM/LP and LPD LSSS.

To achieve these objectives it is necessary to define the probability distributions associated with the uncertainties defined in Section 1.1. The development of these distributions is discussed in Appendix A.

The methods presented in this report are applicable to the following C-E reactors:

Calvert Cliffs Units I and II (Baltimore Gas & Electric Company)

1.4 SUMMARY OF RESULTS

The analytical methods presented in Section 2.0 are used to show that a stochastic simulation of uncertainties associated with the LPD LSSS and TM/LP LSSS results in aggregate uncertainties of [ ], respectively, at a 95/95 probability/confidence limit.

The total uncertainties previously applied to the LPD LSSS and the TM/LP LSSS are approximately [ ], respectively. Therefore the use of the statistical combination of uncertainties provides a reduction in conservatism in the margin to SAFDL of approximately [ ], respectively.

1.5 REFERENCES

1-1 CENPD-199-P, "C-E Setpoint Methodology," April, 1976.

1-2 Docket No. 50-317, "Safety Evaluation by the Office of Nuclear Reactor Regulation," Calvert Cliffs Unit 1 Cycle 3, June 30, 1978.

TABLE 1-1

NSSS PARAMETERS AFFECTING FUEL DESIGN LIMITS

DNBR

1. CORE POWER
2. AXIAL POWER DISTRIBUTION
3. RADIAL POWER DISTRIBUTION
4. AZIMUTHAL TILT MAGNITUDE
5. CORE COOLANT INLET TEMPERATURE
6. PRIMARY COOLANT PRESSURE
7. PRIMARY COOLANT MASS FLOW

LINEAR HEAT RATE

1. CORE POWER
2. AXIAL POWER DISTRIBUTION
3. RADIAL POWER DISTRIBUTION
4. AZIMUTHAL TILT MAGNITUDE

2.0 ANALYSIS

2.1 GENERAL

The following sections provide a description of the analyses performed to statistically combine uncertainties associated with the DNB LSSS and the LPD LSSS. The technique involves use of the computer code SIGMA (Reference 2-1) to select data for the stochastic simulation of the TM/LP and LPD calculations. The bases for the individual uncertainties are presented in Appendix A. The stochastic simulation techniques are described below.

2.2 OBJECTIVES OF ANALYSIS

The objectives of the analyses presented in this section are:

1. To document the stochastic simulation techniques for combining the uncertainties associated with the TM/LP LSSS and the LPD LSSS,

2. To determine the 95/95 probability/confidence limit uncertainty factor to be applied in calculating the TM/LP LSSS and LPD LSSS.

2.3 ANALYTICAL TECHNIQUES

2.3.1 General Strategy

The stochastic simulation code used for the statistical combination of uncertainties associated with the TM/LP LSSS and the LPD LSSS is the computer code SIGMA.

SIGMA produces the dependent variable probability histogram for a number of independent variables. Each of the independent variables has a specified probability distribution associated with it. This is illustrated in Figure 2-1.

The theoretical bases upon which this code depends are those involving the Monte-Carlo and Stratified Sampling Techniques. The functional relationship between the dependent variable and the independent variables depends on the safety system under consideration. For each independent variable a set of data points is generated corresponding to the probability distribution associated with that independent variable. The resulting data set associated with each independent variable is then randomized. Finally the first data point in each data set is selected and all are combined according to the appropriate functional relationship. Combining these randomized independent variables in accordance with the appropriate functional relationship results in a calculated value of a dependent variable. This process is continued until all data in each data set have been used and the resultant dependant variable probability histogram has been generated. The ratio of the mean value of the dependent variable to the lower 95/95 probability/ confidence limit value is the quantity of interest for a lower limit.

The analyses considered in excess of two thousand (2000) power distributions approximately equally distributed at three times in life (BOC, MOC, EOC) for a typical reload cycle depletion. These power distributions were used in the determination of the 95/35 probability/confidence limit uncertainty factors. Power distributions were generated using xenon distributions and CEA configurations that could occur during steady state operation, load maneuvers and uncontrolled axial xenon oscillations in a manner similar to that used for determination of trip setpoints.

2.3.2 TM/LP Stochastic Simulation

For the TM/LP LSSS, DNB overpower (P_{fdn}) is the dependent variable of interest. The core coolant inlet temperature, reactor coolant system pressure, RCS coolant flow rate, peripheral axial shape index and integrated radial peaking factor are the independent variable of interest. CETOP (Reference 2-7), which is based on TORC/CE-1 (References 2-2, 2-3), is the model used to determine the functional relationship between the dependent variable and the independent variables. The probability distributions of uncertainties associated with the independent variable are discussed in Appendix A.

Figure 2-2 is a flow chart representing the stochastic simulation of the DNB limits. The independent variables and their uncertainties are input to SIGMA. Each data set generated by SIGMA is evaluated with CETOP until a P_{fdn} probability distribution is generated. The ratio of the mean value of P_{fdn} to the lower 95/95 value of P_{fdn} is the quantity of interest for evaluating a lower limit.

The core coolant inlet temperature range of interest for the DNB LSSS stochastic simulation is bounded by the loci of the core power and core coolant inlet temperatures corresponding to:

1. the temperature at which the secondary safety valves open; and
2. the temperature at which the low secondary pressure trip occurs.

The reactor coolant system pressure range of interest for the DNB LSSS stochastic simulation is bounded by

1. the value of the high pressurizer pressure trip setpoint; and
2. the lower pressure limit of the thermal margin/low pressure trip.

The details of the specific TM/LP stochastic simulations performed are presented in Section 2.4.

2.3.3 Local Power Density Stochastic Simulation

For the LPD LSSS, the power to fuel design limit on linear heat rate (P_{fdl}) is the dependent variable of interest. The peripheral axial shape index and 3-D peak are the independent variables of interest. The functional relationship between the dependent variable and the independent variables is (Reference 2-4):

$$P_{fdl} = \frac{(Wclm)\ (100)}{(Fq)\ (Wavg)} \qquad (2\text{-}1)$$

where:

- Wclm - peak generated linear heat rate limit representing centerline fuel melt
- Wavg - core average generated linear heat rate at rated power
- Fq - synthesized core power peak.

The probability distributions of each of the uncertainties associated with the independent variables are discussed in Appendix A.

Figure 2-3 is a flow chart representing the stochastic simulation of the LPD LSSS. The independent variables and their uncertainties are input to SIGMA. Each data set generated by SIGMA is input to the functional relationship defined above until a P_{fdl} probability distribution is generated. The ratio of the mean value of P_{fdl} to the lower 95/95 value of P_{fdl} is the quantity of interest.

The details of the specific LPD LSSS stochastic simulation performed are presented in section 2.4.

2.4 ANALYSES PERFORMED

2.4.1 Thermal Margin/Low Pressure LSSS Uncertainty Analysis

In order to combine the uncertainties as shown in Figure 2-2 the stochastic simulation sequence shown in Figure 2-4 was used. Distributions of the following parameter uncertainties are input to the SIGMA sampling module:

[

]

At each selected value of peripheral axial shape index (I_p) the representative axial power distribution is read from the data file. A series of simulation trials (500-1000) is run at this I_p. Each simulation trial uses one sampled value from each parameter distribution.

2.4.1.1 Sampling Module SIGMA

The values of input parameters selected for simulation trials are representative of the actual distribution of parameter values. The SIGMA sampling module performs this data selection using Latin Hypercube Sampling (LHS). (Reference 2-5)

LHS is a stratified sampling scheme that covers the range of the independent variables with a minimum of simulation data points. Distributional characteristics are input to SIGMA [

]. In LHS the range of parameter variation is divided into equal probability intervals. In each interval a point is selected at random from the distribution.

The specific sampling procedure used in this analysis is discussed.

The specific sampling procedure used in this analysis is discussed.

The sampled values for each interval are stored in an array. To generate sets of input values, SIGMA selects intervals at random from each variable using each interval only once in a simulation.

2.4.1.2 Axial Shape Index Calculation

The axial shape seen by the excore detectors is related to the core average axial shape provided by QUIX (Reference 2-6) by several factors. These factors are obtained by calculation or measurement and are subject to some uncertainty. A 20-node core average axial shape is selected from [

]. The core average axial shape index, $\bar{I}$, is calculated from this shape.

$$\bar{I} = \frac{L - U}{L + U} ; \qquad U = \sum_{J=11}^{20} \bar{P}(J) \qquad (2\text{-}9)$$

(2-10)

$$L = \sum_{J=1}^{10} \bar{P}(J) \qquad (2\text{-}11)$$

To relate this to the peripheral shape index inferred by the excores, the following relation is used:

[

] (2-12)

[ ] have uncertainties associated with them. These uncertainties were used in SIGMA to generate representative values of [ ]. Using these values, corresponding values of Ip are computed to obtain a distribution of Ip.

Uncertainties in Ip affect the margin calculation by affecting the trip point selected by the on-line calculators. To account for this, the standard deviation of the distribution of Ip is converted to overpower units using a conservative value of the sensitivity of overpower to Ip. Thus the standard deviation in overpower, $\sigma(B_{opm})$ is

$$\left[\qquad\qquad\right] \tag{2-13}$$

This uncertainty in overpower due to shape index uncertainties is combined with other factors as detailed under Combination of Uncertainties (2.4.1.5).

2.4.1.3 Processing Uncertainties

The Thermal Margin/Low Pressure (TM/LP) trip calculator receives inputs of hot and cold leg temperatures and Ip. It uses these values and the precalculated setpoint relation to produce a low pressure trip point. [ ] methodology is used to estimate the uncertainty due to electronic processing in this result. This estimated standard deviation in the low pressure trip point is calculated for mean values of hot and cold leg temperatures and Ip. To produce the pressure equivalent of the processing uncertainty, pressure values are sampled from [ ] the processing uncertainty for the low pressure trip.

2.4.1.4 Overpower Calculation with Respect to DNBR

Overpower limits due to reactor thermal-hydraulic conditions are determined by the code CETOP (Reference 2-7), which uses the TORC/CE-1 correlation.

CETOP accepts values of pressure, inlet temperature, axial shape, core coolant flow, and radial peaking factor, and returns an overpower limit. In the simulation sequence, the input array produced by SIGMA containing values of CETOP input parameters is modified by adding an adjustment to the pressure value. [

]. The modified pressure value, along with the other parameter values, are input to CETOP, and the resultant overpower value is available for combination with other overpower modifiers.

2.4.1.5 Combination of Uncertainties

During each simulation trial k, the value of DNB overpower produced by CETOP is modified by additional uncertainty values to produce a final overpower value. The final value is given by

[

]

After all simulation trials are run a distribution in overpower is produced for each specific axial power distribution under study, incorporating all uncertainties under consideration.

2.4.2 Local Power Density LSSS Uncertainty Analysis

The stochastic simulation procedure shown in Figure 2.5 was used to implement the calculational sequence outlined in Figure 2.3. The following distributions of parameter uncertainties are input to SIGMA:

[

]

The SIGMA sampling module is described in Section 2.4.1.1.

2.4.2.1 Overpower Calculation with Respect to Linear Heat Rate

For this calculation, ordered pairs of P_{fdl} and $\bar{I}$ values are input to the code. These are obtained from the lower bound of all the "flyspeck" points of the QUIX calculation. [

] Thus the value of P_{fdl} from a simulation run, P_{fdl_h}, is

[

] (2-15)

The value of [ ] is obtained from SIGMA for each simulation trial.

2.4.2.2 ASI Calculational and Processing Uncertainties

The $\bar{I}$ used in the linear heat rate simulation is converted to a peripheral shape index Ip as outlined in Section 2.4.1. If this Ip were generated from the excore detector signals, it would be subject to electronic processing uncertainties. The uncertainty in the simulated value of Ip is

evaluated by a [ ] methodology to estimate the uncertainty due to processing. Values of Ip and mean hot and cold leg temperatures are evaluated to produce a one standard deviation value in Ip due to processing uncertainties.

[ ]

This calculation from $\bar{I}$ to ΔB_{opm} is performed once for each simulation trial.

2.4.2.3 Combination of Uncertainties

For each simulation trial, [ ] the modified overpower value $^{P}fdl_{h}$. Thus, the LHR overpower including uncertainties, $^{B}LHR_{h}$, is

[ ] (2-16)

Over many simulation trials, the required distribution on overpower is built up for each value of ASI incorporating the uncertainties under consideration.

2.5 REFERENCES

2-1 F. J. Berte, "The Application of Monte Carlo and Bayesian Probability Techniques to Flow Prediction and Determination," TIS-5122, February, 1977.

2-2 "TORC Code: A Computer Code for Determining the Thermal Margin of a Reactor Core", CENPD-161-P, July, 1975.

2-3 "TORC Code: Verification and Simplified Modeling Methods", CENPD-206-P, January, 1977.

2-4 CENPD-199-P, "C-E Setpoint Methodology," April, 1976.

2-5 McKay, M. D., et al., "Report on the Application of Statistical Techniques to the Analysis of Computer Codes," LA-NUREG-6526-MS, Los Alamos Scientific Laboratory, October, 1976.

2-6 System 80 PSAR, CESSAR, Volume 1, Appendix 4A, Amendment No. 3, June 3, 1974.

2-7 C. Chiu, J. F. Church, "Three Dimensional Lumped Subchannel Model and Prediction-Correction Numerical Method for Thermal Margin Analysis of PWR Cores," TIS-6191, June, 1979.

BALTIMORE GAS & ELECTRIC CO.
Calvert Cliffs Nuclear Power Plant

STOCHASTIC SIMULATION METHODOLOGY

Figure 2-1

BALTIMORE GAS & ELECTRIC CO.
Calvert Cliffs Nuclear Power Plant

STOCHASTIC SIMULATION OF THE DNB LIMITS

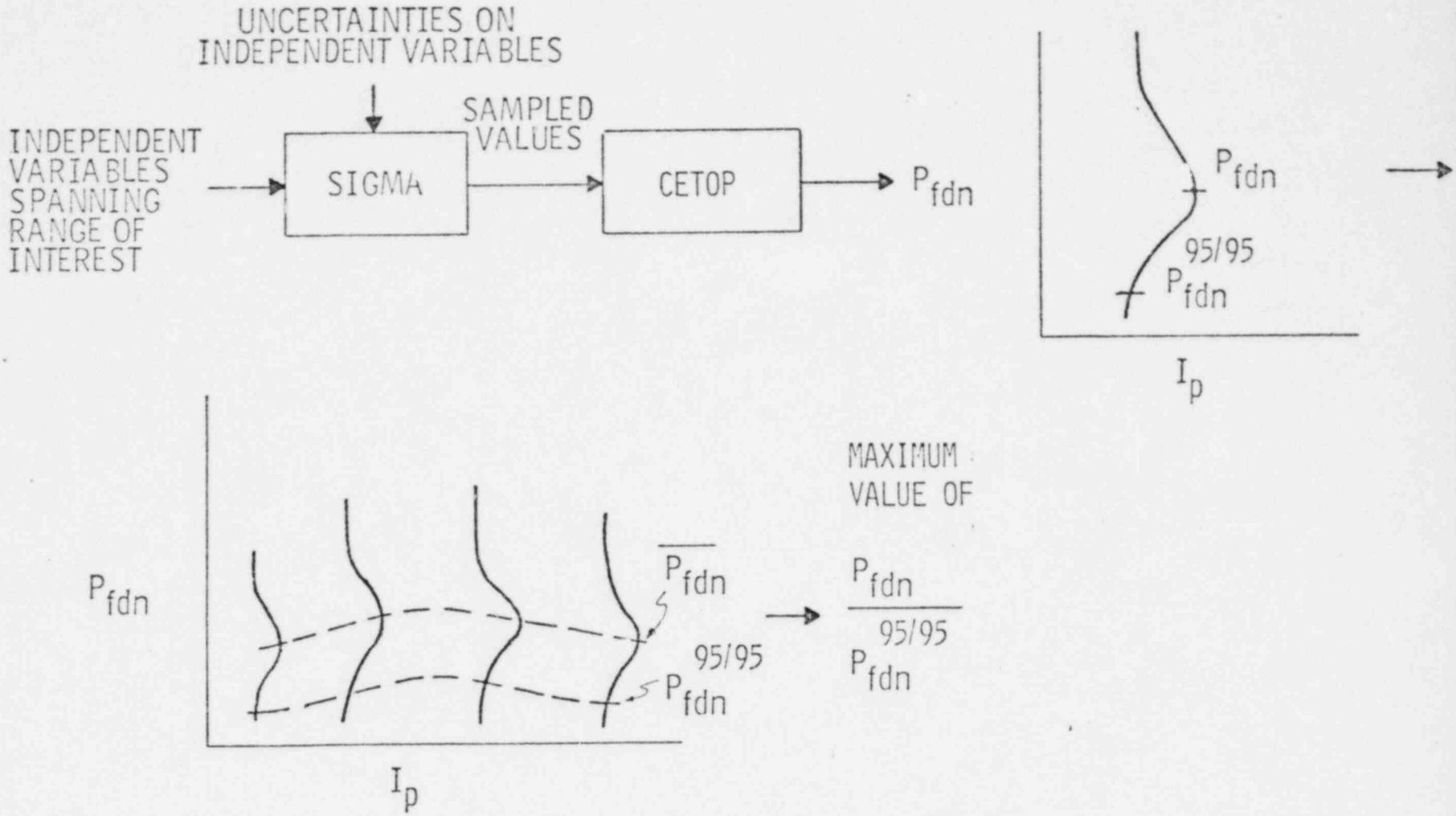

Figure 2-2

BALTIMORE GAS & ELECTRIC CO.
Calvert Cliffs Nuclear Power Plant

STOCHASTIC SIMULATION OF THE LPD LSSS

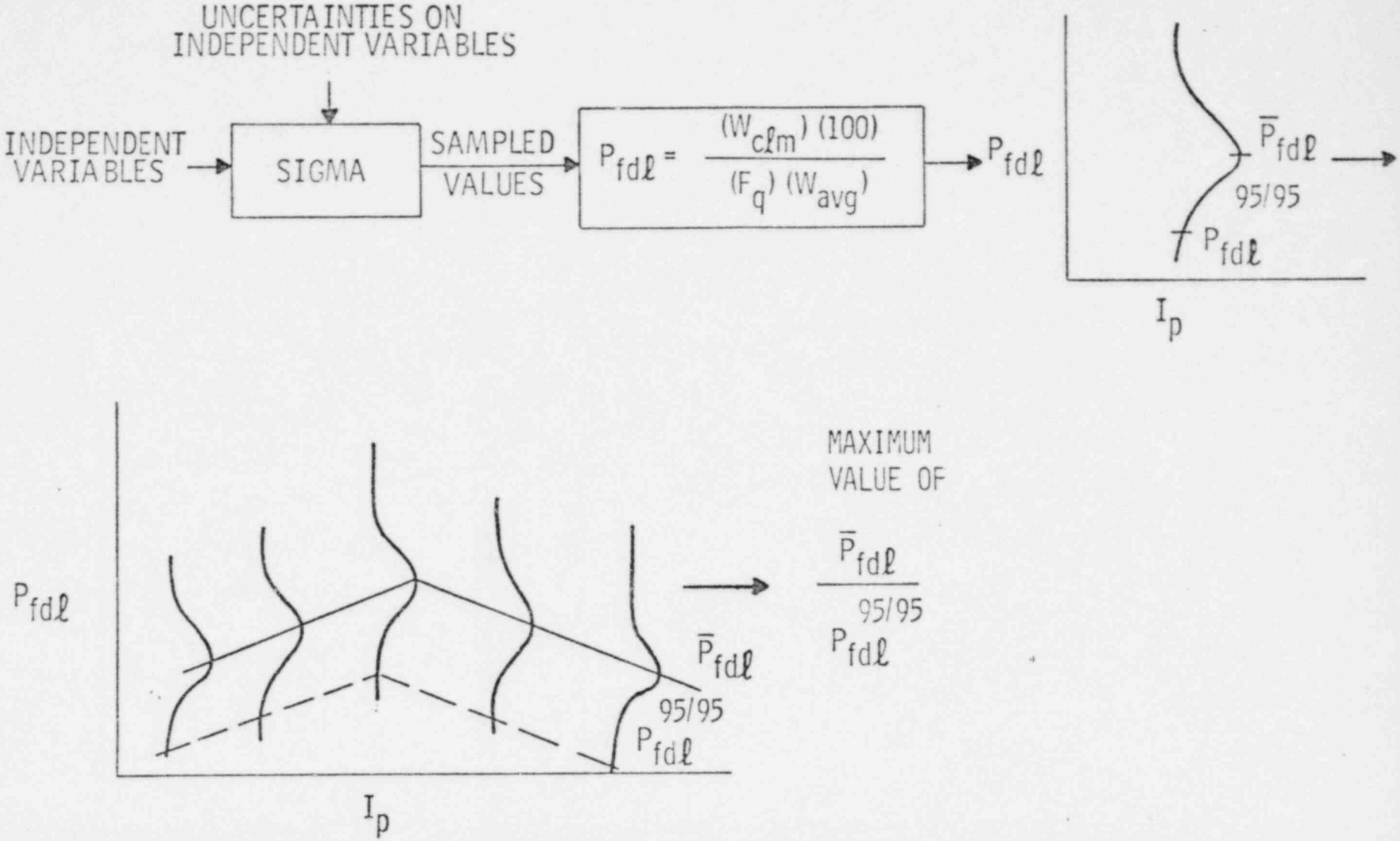

Figure 2-3

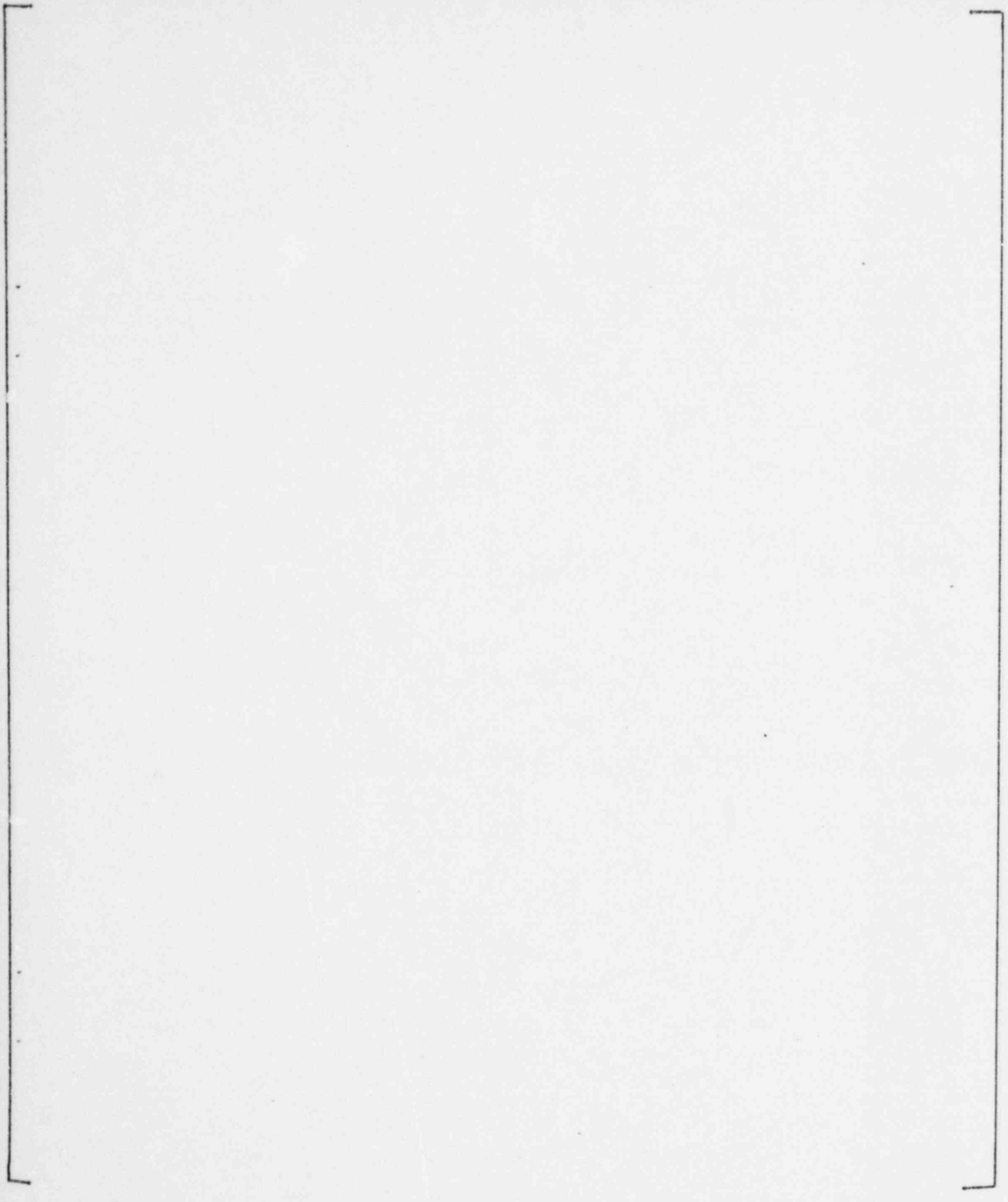

BALTIMORE GAS & ELECTRIC CO. Calvert Cliffs Nuclear Power Plant	THERMAL MARGIN UNCERTAINTY ANALYSIS	Figure 2-4

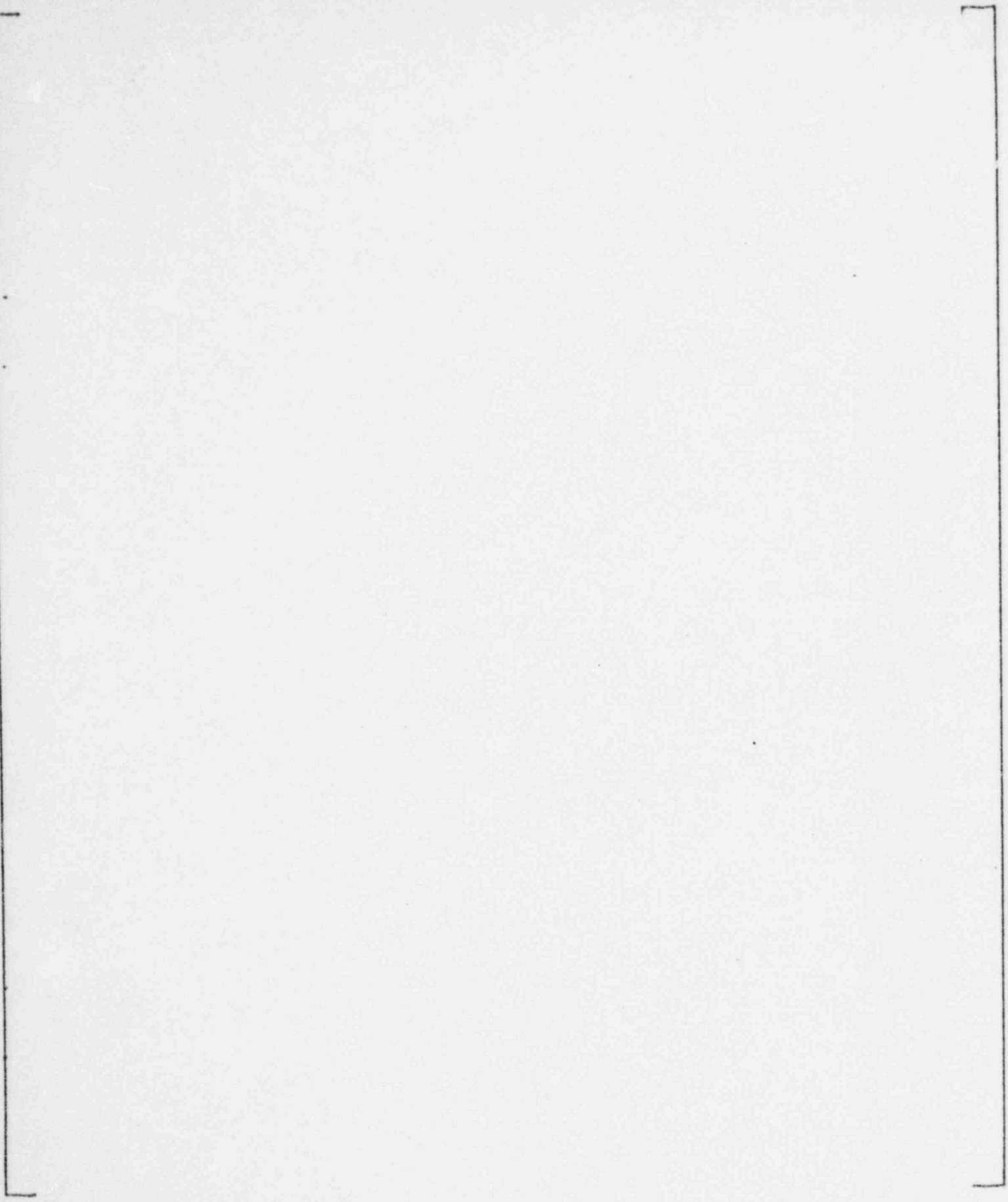

BALTIMORE GAS & ELECTRIC CO. Calvert Cliffs Nuclear Power Plant	LINEAR HEAT RATE UNCERTAINTY ANALYSIS	Figure 2-5

3.0 RESULTS AND CONCLUSTIONS

3.1 RESULTS OF ANALYSES

The analytical methods presented in Section 2 have been used to show that a stochastic simulation of uncertainties associated with the Local Power Density LSSS and the TM/LP LSSS results in aggregate uncertainties of [ ], respectively, at a 95/95 probability/confidence limit.

Table 3-1 shows the values of the individual uncertainties which were statistically combined to yield the above aggregates. Appendix A contains a further discussion of the bases for these individual uncertainties.

The aggregate uncertainties are in units of percent overpower (P_{fdl} and P_{fdn}) and are applied in the generation of the LPD and TM/LP LSSS as discussed below.

3.1.1 Local Power Density LSSS

The fuel design limit on linear heat rate corresponding to fuel centerline melting is represented by the ordered pairs (P_{fdl}, I_p). A lower bound is drawn under the "flyspeck" data such that all the core power distributions analyzed are accommodated. This lower bound is reduced by the applicable uncertainties and allowances to generate the LSSS as follows:

[ ] (3-1)

(3-2)

where:

B_{LHR}^{LSSS} - Power limit for LHR LSSS

SMLS - Statistically Combined Uncertainties Applicable to the Local Power Density LSSS

TPD - Allowance for Transient Power Decalibration

ASI^{LSSS}_{LHR} - Axial shape index associated with B^{LSSS}_{LHR}.

3.1.2 TM/LP LSSS

The fuel design limit on DNBR for the TM/LP LSSS is represented by a combination of the ordered pairs (P_{fdn}, I_p) and the DNB thermal margin limit lines. A lower bound is drawn under the "flyspeck" data such that all the core power distributions analyzed are accommodated. This lower bound is reduced by applicable uncertainties as follows:

[ ] (3-3)

(3-4)

where:

Bopm - Available overpower margin

SMDS - Statistically Combined Uncertainties Applicable to the TM/LP LSSS

ASI_{DNB} - Axial shape index associated with B_{opm}.

Both components of the TM/LP LSSS can be represented by the following equations:

[(3-5)

(3-6)

(3-7)]

[ ] (3-8)

where:

α, β, γ - Coefficients

B_{DNB} - Core power, % of rated power

$P_{var}^{LSSS,DNB}$ - Variable pressure to achieve DNB at the LSSS Limit including uncertainties

RDT - Pressure Equivalent of the Total Trip Unit Processing Delay Time for the DBE Exhibiting the Most Rapid Approach to the SAFDL on DNBR.

B_{DNB}^{LSSS} - Power level after inclusion of DNB LSSS uncertainties and allowances.

TPD - Allowance for Transient Power Decalibration

$T_{in}^{LSSS,DNB}$ - Core inlet temperature associated with $P_{var}^{LSSS,DNB}$

T_{in}^{DNB} - Inlet coolant temperature used in the calculation of (P_{fdn}, Ip) ordered pairs of data.

3.2 IMPACT ON MARGIN TO SAFDL

The motivation for using a statistical combination of uncertainties is to improve NSSS performance through a reduction in the analytical conservatism in the margin to the SAFDL. This section contains a discussion of the margin obtainable through a reduction in this conservatism.

Table 3-2 lists the uncertainty values previously used on the plants included in this analysis. The approximate worth of each of these uncertainties in terms of percent overpower margin (P_{fdl}, P_{fdn}) is also shown.

The total uncertainties previously applied to the Local Power Density LSSS and the TM/LP LSSS are approximately [ ], respectively. The uncertainties resulting from the application of the statistical combination of uncertainties program are approximately [ ]. The use of the statistical combination of uncertainties provides a reduction in conservatism in the margin to SAFDL of approximately [ ], respectively.

Although the conservatism in the margin to SAFDL has been reduced, a high degree of assurance remains that the SAFDL will not be violated.

3.3 REFERENCES

3-1 "TORC Code: A Computer Code for Determining the Thermal Margin of a Reactor Core", CENPD-161-P, July, 1975.

3-2 "TORC Code: Verification and Simplified Modeling Methods", CENPD-206-P, January, 1977.

3-3 CENPD-199-P, "C-E Setpoint Methodology," April, 1976.

TABLE 3-1

UNCERTAINTIES ASSOCIATED WITH THE LOCAL POWER DENSITY LSSS AND THE TM/LP LSSS

Uncertainty*	LPD LSSS	DNB LSSS	
Core power (% of rated power)	± 2%	± 2%	
Primary coolant mass flow (% design)	NA	[	**
Primary coolant pressure (psid)	NA		**
Core coolant inlet temperature (°F)	NA	]	**
Power distribution (peaking factor)	7%	6%	
1. Separability (asiu)	See Table 1 of Appendix A1		
2. Calibration (asiu)	[		]
3. Shape Annealing (asiu)			
4. Monitoring system processing ((asiu)	]		

Notes: *For complete description of these uncertainties, see Appendix A.

**[ ] values

TABLE 3-2

IMPACT OF STATISTICAL COMBINATION OF

UNCERTAINTIES ON MARGIN TO SAFDL

Uncertainty	Value	Approximate Values of Equivalent Operpower Margin (%) DNB LSSS	LPD LSSS
Power	2% of rated	[	
Core coolant Inlet			
Temperature	2 °F		
Reactor coolant system			
Pressure	22 psid		
Axial shape index:			
Separability	[ ]		
Shape Annealing	[ ]		
Calibration	[ ]		
Reactor coolant system			
Flow	[ ]		
Peaking factors	6% DNB, 7% LPD		
Equipment processing:			
DNB LSSS	[ ]		
LPD LSSS	[ ]		
	Total		
Less credit for statistics			
Total Uncertainty Applied Previously			
Total Uncertainty Statistically Combined			
Net Margin Gain			]

APPENDIX A

Basis for Uncertainties Used in Statistical Combination of Uncertainties

A1

Axial Shape Index Uncertainties

LIST OF TABLES

LIST OF FIGURES

Appendix A1

A1.1 Objectives of this Analysis

The four peripheral shape index uncertainties which are incorporated into the setpoint analyses are: 1) the Separability Uncertainty, 2) the Calibration Uncertainty, 3) the Shape Annealing Factor Uncertainty, and 4) the Processing Uncertainty (uncertainties in the electronic processing of excore detector signals). Prior to the development of the methodology to combine these uncertainties statistically, they were combined additively to yield a net uncertainty (Reference A1-1). The purpose of this part of the SCU program is to develop the data base necessary to support a procedure for statistically combining these four components of the axial shape index uncertainty. Table 1 shows the values of the uncertainties developed in this program.

A1.2 General Strategy

Each of the components of the axial shape index uncertainty is investigated in this Appendix in order to justify their statistical combination.

The Separability Uncertainty accounts for the difference between the core average axial shape index and the peripheral axial shape index. This uncertainty has four components:

1. [ ]
2. [ ]
3. [ ]
4. [ ]

The Calibration Uncertainty accounts for errors introducted into the protection system when the excore detector system is periodically adjusted to match measured parameters of the core's power distributon.

The Shape Annealing Factor Uncertainty accounts for the error in the measurement of the shape annealing factor.

The Processing Uncertainty accounts for the uncertainty in Ip calculated by the protection system. This uncertainty is taken into account by its explicit representation in the stochastic simulation procedure used to statistically combine al the uncertainties.

A1.3 Specific Uncertainty Evaluations

A1.3.1 Separability Uncertainty

The Separability Uncertainty is a calculational uncertainty. It is the uncertainty associated with inferring a peripheral shape index, Ip, from a given known core average shape index $\bar{I}$. The one dimensional shape analysis used in the development of setpoints correlates the power to centerline melt (P_{fdl}) and the power to DNB, (P_{fdn}) to the core average axial shape. Since the excore detectors respond only to the power distribution near the periphery of the core, a calculated relationship is needed between $\bar{I}$ and Ip. This relationship, represented in the setpoint development by incorporation of the rod shadowing factors in QUIX (Reference A1-2), is currently calculated by means of the three dimensional code ROCS (Reference A1-3). The uncertainty in this calculation is the Separability Uncertainty.

The Separability Uncertainty consists of four components: [

.] The components of the Separability Uncertainty are discussed in detail below.

A1.3.1.1 [ ]

[

Definition of the first component of the separability uncertainty.

]

[

]

Rod Shadowing Factor Method

The peripheral axial shape index, Ip, is defined in the following manner:

$$I_p = \frac{D_L - D_U}{D_L + D_U} \qquad \text{(A1-1)}$$

where

$$D_U = \int_{H/2}^{H} dx \; R(x) \bar{P}(x) \qquad \text{(A1-2)}$$

$$D_L = \int_{0}^{H/2} dx \; R(x) \bar{P}(x) \qquad \text{(A1-3)}$$

where D_U, D_L are the powers at the periphery of the upper and lower half of the core, respectively.

$\bar{P}(x)$ is the core average power distribution

$R(x)$ is the rod shadowing factor for the rod configuration inserted at position x.

H is the height of the core.

The rod shadowing factors are derived from the product of rodded and unrodded 2D power distributions and the assembly weighting factors, which account for the contribution of each assembly to the excore detector response to a given power distribution.

[

]

Assembly Weighting Factor Method

The Assembly Weighting Factor (AWF) method consists of the following calculation of Ip:

$$I_p = \frac{\Sigma_i W_i P_i I_i}{\Sigma_i W_i P_i} \qquad \text{(A1-4)}$$

where P_i is the axially integrated power of fuel assembly i

I_i is the axial shape index of assembly i

W_i is the weighting factor of assembly i

The W_i values are computed for those core edge assemblies which are the principal source of the excore detector's response.

The result of this procedure is [

].

Analyses have determined this uncertainty and have shown it to be essentially [ ] This component of the separability uncertainty is as shown in Table 1 along with the other components.

A1.3.1.2 [ ]

[Definition of the second component of the separability uncertainty.]

[.] A review of previous cycles shows that [ ] Ip is dependent on rod bank insertion. The [ ] is rod bank insertion dependent. A [ ] fit of the calculated data was performed to determine the mean which is shown in Table 2. An error analysis performed on the difference between the calculated data and the mean shows that [t .] (see Table 1).

A1.3.1.3 [ ]

The third component in the Separability Uncertainty consists of [ ]. The AWF method is described in section A1.3.1.1.

[

Definition of the third component of the separability uncertainty.

]

A1.3.1.4 [ ]

The fourth component of the Separability Uncertainty consists of the [

] the uncertainty in the calculated power distribution also results in a component of the Separability Uncertainty.

[

Definition of the forth component of the separability uncertainty.

]

[ ]

[

]. The result is as follows:

[ ] (A1-5)

Since the above result also [

].

A1.3.2 Uncertainty on Ip

Calibration of the excore detectors relative to the axial shape index as measured by [

] The components of this measurement uncertainty consist of the uncertainty in [

] modeling the reactor power distribution.

The calibration is performed [

] This calibration is done near an ASI of zero so that accuracy of the shape annealing factor has minimal impact on the calibration result.

The measurement uncertainty on $\bar{I}$ is analyzed herein by [

] Differences between $\bar{I}$ [ ] were studied to determine uncertainties statistically. The mean and standard deviation of the respective differences for each cycle were calculated, after which the data were examined to determine whether the cyle by cycle data could be pooled.

[

Description of data used.
Results of analysis.

]

Table 3 shows the standard deviations of the [ ] comparison of $\bar{I}$. The pooled cycles which formed the basis of the above uncertainty data is also indicated in Table 3.

A1.3.3 Shape Annealing Factor Uncertainty

The shape annealing factor, α, is an experimentally measured value which relates the external axial shape index I_e to the peripheral axial shape index.

$$I_p = \alpha I_e \qquad \text{(A1-6)}$$

This factor accounts for the fact that the excore detectors respond to the power in both the upper and the lower portion of the core. This signal mixing yields shape annealing factors which are larger for detectors which are far from the periphery than for detectors which are near the periphery. The theoretical lower limit of α is unity.

The shape annealing factor is measured [ ]by inducing a xenon oscillation in the core and measuring the external shape index of the j^{th} excore channel(I_e^j) along with the internal axial shape index $\bar{I}$ as measured by the CECOR system using incore instruments. The [ ] slope of $\bar{I}$ versus I_e^j is the shape annealing factor. At the beginning of life $\bar{I}$ is assumed to be equal to I_p. [

] as discussed above.

Measured values of the shape annealing factor are shown in Table 4 for various C-E operating reactors.

An error analysis was performed on this data to determine the deviation of each value of α from the average values for a given plant and a given channel. The error analysis was performed on [

] The data is presented in Table 5 for all plants except for BG&E Unit 2. For BG&E Unit 2 only one test has been performed and therefore a specific deviation from an average cannot be defined.

This data was analyzed for pooling using the Bartlett test, and for normality using the W test. It was found that the pooled standard deviation [ ] and that the corresponding Bartlett statistic [ ] This is to be compared with a theoretical Bartlett statistic at the upper 5% significance level equal to[ ]. This means that the above data is consistent with the assumption that all are samples from the same parent population. [

]

[

]

Since the assumption of pooling has been shown to be warranted, [

]

tolerance limit can be evaluated. Results show that [

] This K factor times the above standard deviation yields a 95/95 tolerance limit

[ ]

A1.3.4 Processing Uncertainty

The Processing Uncertainty is discussed in Appendix A3.

A1.4 [ ] of the Peripheral Shape Index Uncertainties

The following [ ] have been identified in the development of peripheral shape index uncertainties.

Discussion of the components of the peripheral shape index uncertainties.

[Discussion of the components of the peripheral shape index uncertainties.]

Equation A1-10 is an identity. Equation A1-11 follows from the assumption that [

].

Equation A1-12 and the results summarized in Table 1 are used in the stochastic simulator described in Section 2.4 of this report.

A1.5 References

A1-1 "C-E Setpoint Methodology," CENPD-199-P, April, 1976.

A1-2 System 80 PSAR, CESSAR, Volume 1, Appendix 4A, Amendment No. 3, June 3, 1974.

A1-3 BG&E Application for Cycle 4 Reload, AE Lundvall (BG&E) to R. W. Reid (NRC), February 23, 1979.

A1-4 "INCA, Method of Analyzing In-Core Detector Data in Power Reactors," CENPD-145-P, April, 1975.

A1-5 "Evaluation of Uncertainty in the Nuclear Form Factor Measured by Self-Powered Fixed In-Core Detector Systems," CENPD-153, August, 1974.

Table 1

Uncertainty [ ] Components

for the Evaluation of the

Peripheral Shape Index(1)

	Kσ 95/95 (asiu)	K(f)(2)	[ ]
I. Separability Uncertainty	[		]
II. Calibration Uncertainty(n)	[		]
III. Shape Annealing Uncertainty(n)			
IV. Processing Uncertainty(n)			

Notes On Table 1

(1) All components of the peripheral shape index have been tested for normality, [ ]

(2) f = degrees of freedom.

(3) [ ]

(4) This $K\sigma^{95/95}$ is for consistent sets of input data used by the uncertainty processors.

Table 2

[

]

Rod Bank Insertion	[Generic QUIX Bias, asiu]
All Rods Out (ARO)	[ ]
Reg Bank 1 (20%)	
Reg Bank 1 (40%)	
Reg Bank 1 (60%)	
Reg Bank 1 (80%), Reg Bank 2 (20%)	
Reg Bank 1 (100%),Reg Bank 2 (40%)	
Reg Bank 1 (100%),Reg Bank 2 (60%)	
Reg Bank 1 (100%),Reg Bank 2 (80%), Reg Bank 3 (20%)	
Reg Bank 1 (100%),Reg Bank 2 (100%), Reg Bank 3 (40%)	
Reg Bank 1 (100%),Reg Bank 2 (100%), Reg Bank 3 (60%)	

Table 3

[ ]

Reactor	Number of Data Points	Mean Value, asiu	Standard Deviation, asiu
1. St. Lucie I Cycle 1	[		]
2. St. Lucie I Cycle 2			
3. Calvert Cliffs I Cycle 1			
4. Calvert Cliffs I Cycle 2			
5. Calvert Cliffs I Cycle 3			
6. Calvert Cliffs II Cycle 1			
7. Calvert Cliffs II Cycle 2			
8. Millstone II Cycle 1			
9. Millstone II Cycle 2			

[

]

Table 4

Measured Values of Shape Annealing Factors

St. Lucie 1

Channel	Cycle 1 June 1976 50% Power	Cycle 1A Jan 1977 50% Power	Cycle 2 June 1978 80% Power	Cycle 3* June 20, 1979 80% Power
[redacted]				

*Note that a new streaming shield was placed in St. Lucie I at EOC2.

This new streaming shield changed the shape annealing factors.

Calvert Cliffs Unit 1

Channel	Cycle 1 Feb 1975 80% Power	Cycle 2 April 7, 1977 50% Power
[redacted]		

Table 4 (Continued)

Calvert Cliffs Unit 2

Channel	Cycle 1 Dec 27, 1976 50% Power
[redacted]	[redacted]

Millstone Point 2

Channel	Cycle 1 Feb 6-9, 1976 50% Power	Cycle 1 March 11, 1976 80% Power
[redacted]	[redacted]	[redacted]

Table 5

[ ]
Standard Deviation of the Shape
Annealing Factor for Each Channel

Plant & Channel	Number of Degrees of Freedom f	[ ] Standard Deviation per Channel [ ]
St. Lucie 1	[	]
Calvert Cliffs 1		
Millstone Point 2		

BALTIMORE GAS & ELECTRIC CO.
Calvert Cliffs Nuclear Power Plant

Figure A1-1

BALTIMORE GAS & ELECTRIC CO.
Calvert Cliffs Nuclear Power Plant

Figure A1-2

BALTIMORE GAS & ELECTRIC CO.
Calvert Cliffs Nuclear Power Plant

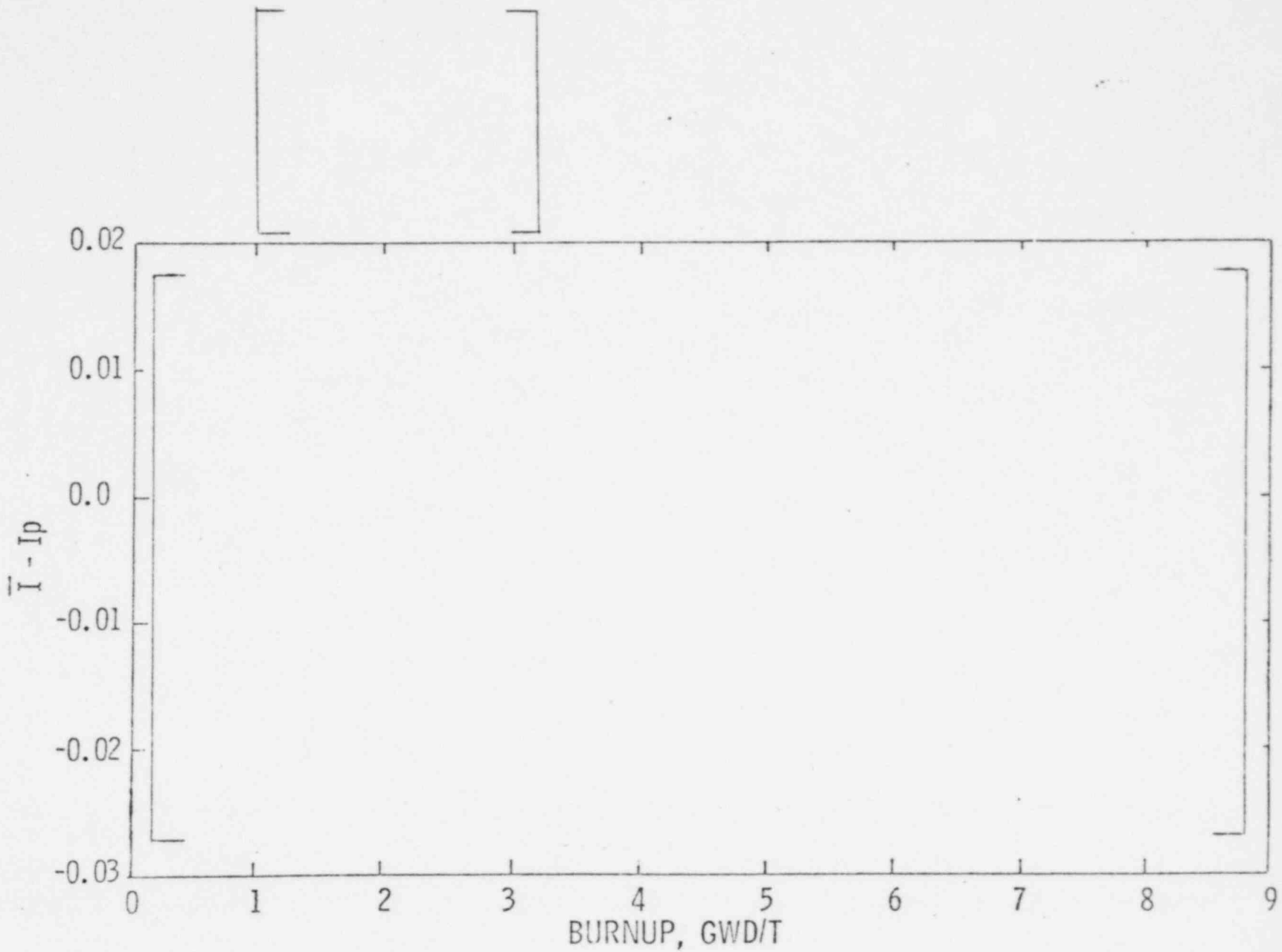

Figure A1-3

A2

Measurement Uncertainties

Appendix A2

A2.1 Basis for Flow Uncertainty

The flow rate was determined by an evaluation of calorimetric data taken from the Calvert Cliffs Nuclear Power Plant at approximately 100% reactor power. Uncertainty in that flow rate was evaluated by examining the uncertainties in each input parameter used in the flow determination. The inputs include hot and cold leg RTD temperatures, system pressure, and core thermal power. The core thermal power is based on a secondary side calorimetric measurement. Each component uncertainty was first evaluated and then the net effect of all instrumentation inaccuracies on calculated flow rate was determined [

]. The resulting overall [ ] uncertainty was found to be [ ] of the flow rate.

A2.2 Monitored Thermal-Hydraulic Parameter Uncertainty Distributions

The uncertainty distributions previously used to characterize the inputs to the safety analyses and setpoint thermal-hydraulics modules were based on highly conservative assumptions. Table 1 outlines these distributions.

It is now possible to refine these distributions using more detailed system analysis and observed plant data. Updated distributions representing more detailed system analysis and measured data from the Calvert Cliffs Nuclear Power Plant have been examined to define specific contributors to the total uncertainty and dependencies between parameters. The uncertainty distributions shown in Table 2 represent the results of this detailed systems analysis.

Measurement of these parameters' uncertainties show both random and nonrandom components which are so small that their most adverse contributions are fully covered by the uncertainties of Table 2. The degree of dependency found is so small that, in conjunction with the size of the evaluated uncertainties, the assumption of independence amoung the parameters of Table 2 is justified. Therefore, for the purposes of the statistical contribution of uncertainties evaluation reported herein, the uncertainties of Table 2 can be used in the stochastic simulation model.

A.2.3 Power Peaking Factor Uncertainties

The 3D Power Peaking Factor Uncertainty (F_Q) and the Integrated Radial Power Peaking Factor Uncertainty (F_R) are currently being re-evaluated in response to NRC questions regarding C-E's uncertainty topical report (Reference A2-1). Pending resolution of these questions and approval of the topical report, C-E will continue to use the values listed in Table 3. These values are used in the stochastic simulator described in this report.

References

A2-1 "Evaluation of Uncertainty in the Nuclear Form Factor Measured by Self-Powered Fixed In-Core Detector Systems" CENPD-153, August 1974.

TABLE 1

Previously Assumed Uncertainty Distributions
on Monitored Thermal/Hydraulic Parameters

Parameter	Distribution
[	]

Note:

[ ]
*This value includes measurement and processing system uncertainties.

TABLE 2

Results of Detailed Systems Analysis
of Monitored Thermal/Hydraulic Parameters

Parameter	Distribution
[	]

Note:

[ ]
*This value is a measurement uncertainty only. Processing system uncertainties are handled separately.

TABLE 3

Peaking Factor Uncertainties

Peaking Factor	Uncertainty (% of Power)
F_R	6.0
F_Q	7.0

A3

Trip System Processing Uncertainties

A3 Trip System Processing Uncertainties

Two types of instrument errors are considered in this analysis. First are those errors that are random in nature. The basic accuracy of an instrument or component falls into this category as it is dependent upon such factors as manufacturing tolerances, etc. Second are those errors that are deterministic and present in approximately the same degree in any equipment built to a given design. Examples of this type of error are changes due to temperature, changes under force loads etc.

The reason for considering two types of errors is that the mathematical techniques for combining errors from several sources differs for each type of error. The deterministic errors are combined using the governing equations and the techniques of ordinary algebra, while the random errors are best combined using probabilistic methods.

The method of determining the random error of an instrumentation loop is based upon two approximations. The first approximation is that the errors of the various pieces of equipment are independent. The second approximation that is used in the analysis is that the equations which define the relationships between the variables in the instrumentation loop can be approximated by the linear terms of a Taylor series expansion. This is a good approximation because the errors are very small in relation to the overall range of the quantities in question and cause only small perturbations about the nominal value.

The procedure followed in calculating the variance consists of obtaining the partial derivatives of the system or instrument equation with respect to each of the variables and evaluating them at the nominal values. These partial derivatives are then used to calculate the variance.

This method of determining the variance of a function of several variables was arrived at without placing any restrictions on the probability distributions of the variables involved, hence the method is generally applicable. Having obtained the variance, its significance can only be interpreted in terms of the distribution to which it applies. The probability distribution of a function that is dependent upon several variables is dependent upon the distribution of those variables. However as the number of variables increases (such as that obtained by using the previously described method), the resulting distribution tends to a normal curve (this is the Central Limit Theorem).

If the probability densities of the variables are reasonably concentrated near the nominal values [

The instrument errors are calculated in the stochastic simulation procedure. In this computerized error analysis, a subprogram is used for each type of module (i.e., power supply, multiplier/divider, adder/subtracter, etc.) Each subprogram accepts the input voltages and errors (in volts) for its module and determines the outputs of the module and their associated errors.

The simulation then goes through the calculator, module by module. As each module is reached, the appropriate subprogram is called. The module inputs are obtained from the outputs of the modules which feed it.

APPENDIX B

Summary of Previous Methods for Combining Uncertainties

Appendix B

The methods previously used for the application of uncertainties to the LSSS are presented in Reference B-1 and are summarized in this Appendix.

B.1 Limiting Safety System Setting on Linear Heat Rate (LPD LSSS)

The fuel design limit on linear heat rate at fuel centerline melt is represented by the ordered pairs (P_{fdl}, I_p). A lower bound is drawn under this "flyspeck" data such that all the core power distributions analyzed are accommodated. Using the previous methodology this lower bound was reduced by the applicable uncertainties and allowances to generate the Local Power Density LSSS as follows:

[ ] (B-1)

(B-2)

where:

T_{AZ} - Azimuthal Tilt Allowance
PU - Uncertainty in predicting local core power at the fuel design limit
BMU - Power measurement uncertainty
SAU - Shape annealing factor uncertainty
RSU - Shape index separability uncertainty
ACU - Axial shape index calibration uncertainty
APU - Processing uncertainty

B.2 Limiting Safety System Setting on DNBR (TM/LP LSSS)

The fuel design limit for the TM/LP trip on DNBR is represented by a combination of the ordered pairs (P_{fdn}, I_p) and the DNB TMLL. A lower bound is drawn under the "flyspeck" data such that all the core power

distributions analyzed are accommodated. Using the previous methodology this lower bound was reduced by applicable uncertainties and allowances as follows:

[ ] (B-3)

[ ] (B-4)

where:

SC - approved partial credit for conservatism in uncertainty application.

Both components of the DNB LSSS were then represented by the following equations:

[ ] (B-5)

[ ] (B-6)

[ ] (B-7)

[ ] (B-8)

where:

RDT - Pressure equivalent of the total trip unit and processing delay time for the DBF exhibiting the most rapid approach to the SAFDL on DNBR

PMU - Pressure measurement uncertainty

TPU - Processing uncertainty

BMU - Power measurement uncertainty

TMU - Temperature measurement uncertainty

REFERENCE

B-1 CENPD-199-P, "C-E Setpoint Methodology," April, 1976